Nonclassical Behavior of Thin-Walled Composite Beams with Closed Cross Sections

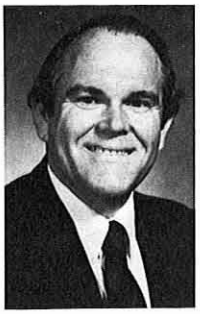

Lawrence W. Rehfield
Professor, Aero. Science and Engineering
Univ. of Calif., Davis

Ali R. Atilgan
NATO Scholar
Post Doctoral Fellow

Dewey H. Hodges
Professor

School of Aerospace Engineering
Georgia Institute of Technology,
Atlanta, Ga.

This paper focuses on two nonclassical effects in the behavior of thin-walled composite beams: elastic bending-shear coupling and restrained torsional warping. These nonclassical effects are clarified and analyzed in some simple examples involving cantilevered beams. First, elastic bending-transverse shear coupling is shown to be important in the analysis of beams designed for extension-twist coupling. It is found that the lateral deflections can be off by more than a factor of two if this coupling is ignored. This coupling stems from plies with off-axis fibers in the beam. The presence of these plies affects significantly the modeling approach (i.e., determination of the constitutive equations) in that transverse shear must appear in the kinematics so that its coupling with bending will be exhibited in the elastic constants. This finding is in accord with "exact" beam theories which develop the beam displacement and cross sectional orientation in terms of six kinematical variables instead of the three or four found in some previously published works on composite blade modeling. A second nonclassical effect, torsional warping rigidity, is shown to be important for certain box beams having a thin-walled, closed cross section. The importance of including these nonclassical phenomena in a complete theory is discussed in light of the magnitude of their effects for various values of configuration parameters.

Introduction

Aerospace vehicle structures are largely composed of thin-walled elements stiffened by beam-like members and are increasingly being made of composite materials. There are certain modeling assumptions that are typically associated with so-called classical analyses of isotropic beams which will not suffice for beams made of composite materials. The usual classical analyses must be revised to include certain nonclassical effects. Two of these nonclassical effects, bending-shear coupling and torsional warping rigidity, are the subjects of the present paper. Here "shear" refers to transverse shear in the sense of Timoshenko theory. While shearing strains and torsional warping rigidity are treated in some classical analyses, the influence of such effects is usually small for isotropic beams. (Exceptions to this include isotropic beams with open cross sections, which are not considered herein, for which warping rigidity is known to be important.) For composites, on the other hand, these effects may not be small. The analysis which follows is intended as a contribution towards understanding theoretical foundations for analysis of composite beams with thin-walled closed cross sections and their physical behavior. We intend furthermore to determine the extent to which bending-shear coupling and torsional warping rigidity are essential elements of such an understanding.

The subject of composite rotor blade modeling was reviewed in Ref. 1. There exist quite general approaches to the determination of sectional constants ranging from powerful finite element methods such as Ref. 2 to simple analytical methods such as Ref. 3. Reference 2 shows that there are two classes of warping involved in the calculation of sectional elastic constants. The particular solution (also called the St. Venant solution) ignores all end effects that arise from restraining the warping. This solution allows the determination of a 6×6 matrix of elastic constants for the blade cross section. Thus, shear deformation must be included in the blade deformation model in order for these constants to contribute to the strain energy.

The homogeneous (or boundary layer) solutions, however, allow the end effects to be treated to a varying degree of accuracy depending on how many of the restrained warping "modes" are retained. Each of these modes has a characteristic length which determines how rapidly its effects decay with the distance from the ends. In order to make use of these solutions in the determination of sectional elastic constants, additional kinematical variables, which serve as amplitudes for their modes,

Presented at the American Helicopter Society National Technical Specialists' Meeting on Advanced Rotorcraft Structures, Oct 25–27, 1988, Williamsburg, Va.

must be incorporated into the deformation model. These additional variables can be the derivatives of existing ones. Subsequent work in Ref. 4 shows that, among the out-of-plane restrained modes, the torsional warping mode is the most significant.

For an arbitrary composite beam the in-plane and out-of-plane St. Venant solutions can be quite significant. When we restrict the discussion to thin-walled beams, however, the St. Venant warping solutions do not significantly affect the stiffness constants (Ref. 5). Thus, a useful contribution to the understanding of composite blade modeling would be to examine a simple thin-walled blade theory including at least the full 6 × 6 matrix of elastic constants while also examining the effects of additional constants associated with the out-of-plane torsional warping.

The simplest theory required to examine the importance of bending-shear coupling and restrained out-of-plane torsional warping is that of Ref. 3, a linear composite beam theory, which serves as the starting point for this study. Results from this theory were shown to agree well with NASTRAN finite element results for the static deformation of a model rotor blade (Ref. 6). Very good correlation between the theory and experiments was also obtained for both box beams (Ref. 7) and circular tubes (Ref. 8). In Ref. 7 Rehfield's theory (Ref. 3) was able to predict strain distribution in the beam cross section. Also, the correlation between Rehfield's theory and the experiment in Ref. 8 was very good.

In this paper, we proceed by first summarizing the basic equations of Rehfield's theory, in which distortion in the plane of the cross section, local shell bending and twisting moments, the hoop stress resultant, and initial twist and curvature are not considered. The significance of the nonclassical effects is evaluated by means of simple examples involving cantilevered beams. The importance of bending-shear coupling is assessed for beams designed for extension-twist coupling. Finally, the importance of restrained torsional warping in composite beams is assessed for a family of thin-walled box beams. The differences relative to isotropic cases are highlighted.

Synopsis of the General Theory

The starting point of our considerations is the linear theory for thin-walled, composite beams developed in Ref. 3. After the kinematics of the theory are summarized, we will then outline development of the equilibrium equations and the force-deformation relationships from the principle of virtual work.

Kinematics

A thin-walled beam with closed, single-cell cross section is shown in Fig. 1. The coordinate direction x is along a straight, but as yet unspecified, reference axis while y and z are the transverse coordinates of the cross section measured from the reference axis. The circumferential coordinate s is taken along the middle surface of the wall. The beam undergoes stretching, bending, twisting, and transverse shearing. Introducing a frame which coincides with the cross section of the undeformed beam, one can decompose the displacement field of the beam into a rigid-body translation and rotation of the frame, and a warping of the cross section relative to that translated and rotated frame. Considering only small displacements and rotations and ignoring distortion of the cross section in its own plane, one can immediately represent the transverse displacement components in the form

$$v = V - z\phi$$

$$w = W + y\phi \tag{1}$$

Here $V = V(x)$ and $W = W(x)$ are transverse components of the displacement at the point where the reference axis passes through a given cross section, and $\phi = \phi(x)$ is the twist angle.

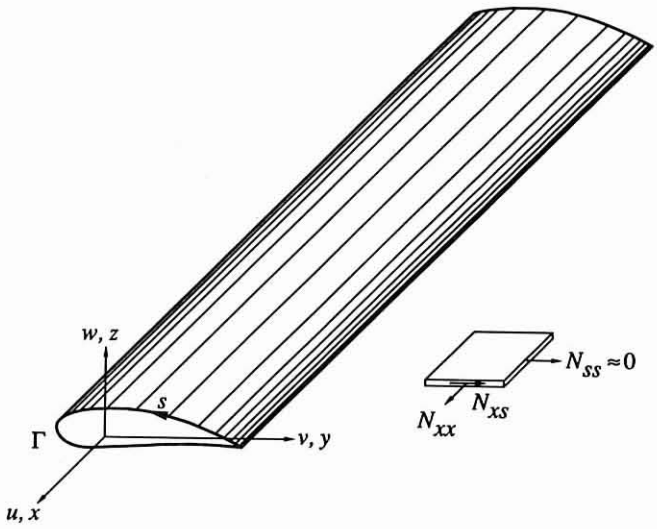

Fig. 1 Schematic of thin-walled beam configuration.

In order to obtain an expression for the axial deflection u, some assumptions must be made concerning the tranverse shear strains. As in the usual theory of torsion for thin-walled beams made of isotropic materials, the shear strain is assumed to be independent of s. Therefore, let $\gamma_{xy} = \gamma_{xy}(x)$ and $\gamma_{xz} = \gamma_{xz}(x)$ be the transverse shear strains of any cross section. They are assumed to be uniform for each cross section so that there is no warp due to transverse shear; that is, a pure transverse shear strain results in a plane cross section. Furthermore, let $\gamma = \gamma(x)$ be the shear strain due to twisting. Therefore, from the strain transformation law and elementary geometrical considerations, the membrane shear strain in the beam wall is given by

$$\gamma_{xs} = \gamma_{xy}\frac{dy}{ds} + \gamma_{xz}\frac{dz}{ds} + \gamma \tag{2}$$

Introducing the position vector $\mathbf{r}$ from the reference axis of the beam to an arbitrary point in the wall of the beam and a unit vector $\mathbf{n}$ normal to the wall at the arbitrary point and directed toward the interior of the cross section, one can express the shear strain in terms of the deformation as

$$\gamma_{xs} = u_{,s} + v_{t,x} \tag{3}$$

where v_t is the tangential component of displacement given by

$$v_t = V\frac{dy}{ds} + W\frac{dz}{ds} - \mathbf{r}\cdot\mathbf{n}\phi \tag{4}$$

Following Ref. 3, one can find the form of the axial displacement component, u, by ignoring any effects of taper along the spanwise direction and by enforcing the continuity condition around the circumference of the cross section. The result is

$$u = U - y\beta_z + z\beta_y + \psi\phi_{,x} \tag{5}$$

where $U = U(x)$ is the axial component of the displacement of the point where the reference axis passes through a given cross section, $\beta_y = \beta_y(x)$ and $\beta_z = \beta_z(x)$ are the cross section rotations, positive in a right-handed sense about the axes y and z, respectively,*

*In other words, U, V, and W are components of the rigid-body displacement of the point in the cross sectional frame where the reference axis passes through it; ϕ, β_y, and β_z are components of the rigid-body rotation of the cross sectional frame.

$$\beta_y = \gamma_{xz} - W_{,x}$$

$$\beta_z = V_{,x} - \gamma_{xy} \tag{6}$$

and ψ is the torsional warping function given by

$$\psi(s) = \frac{2A}{c}s + \int_0^s \mathbf{r}(s^*) \cdot \mathbf{n}(s^*)ds^* \tag{7}$$

which satisfies the condition that $\oint_\Gamma \psi ds = 0$. Here A is the enclosed area of the cross section, $c = \oint_\Gamma ds$ is the circumference, and Γ represents the cross section shape. The axial strain is then obtained as

$$\epsilon_{xx} = U_{,x} - y\beta_{z,x} + z\beta_{y,x} + \psi\phi_{,xx} \tag{8}$$

and the shear strain is

$$\gamma_{xs} = \gamma_{xy}\frac{dy}{ds} + \gamma_{xz}\frac{dz}{ds} + \frac{2A}{c}\phi_{,x} \tag{9}$$

where $U_{,x}$ is the axial strain, and γ_{xy} and γ_{xz} are the shear strains at the beam reference axis, while $\phi_{,x}$, $\beta_{y,x}$, and $\beta_{z,x}$ are the twist and bending curvatures, respectively. $\phi_{,xx}$ is the additional kinematical variable associated with torsional warping. With both shear deformation and torsional warping present in the theory it is possible to examine the roles of these nonclassical effects.

Force-Deformation Analysis by Principle of Virtual Work

For thin-walled beams, local shell bending and twisting moment resultants can be ignored, and thus, the beam reacts external forces by membrane action in the wall. Introducing axial and shear stress resultants, N_{xx} and N_{xs}, respectively, and assuming that there is no internal pressure so that the hoop stress resultant, N_{ss}, can be ignored, one can write the principle of virtual work as

$$\int_0^L \oint_\Gamma (N_{xx}\delta\epsilon_{xx} + N_{xs}\delta\gamma_{xs})dsdx - \delta W = 0 \tag{10}$$

where δW is the virtual work of the external forces. Application of the calculus of variations with the usual assumptions regarding continuity results in the following equations of equilibrium:

$$\begin{aligned} N_{,x} + q_x &= 0 \\ Q_{y,x} + q_y &= 0 \\ Q_{z,x} + q_z &= 0 \\ M_{x,x} - Q_{w,xx} + m_x - q_{w,x} &= 0 \\ M_{y,x} - Q_z + m_y &= 0 \\ M_{z,x} + Q_y + m_z &= 0 \end{aligned} \tag{11}$$

where the generalized internal forces are defined as

$$\oint_\Gamma N_{xx}(1, z, -y, \psi)ds = (N, M_y, M_z, Q_w)$$

$$\oint_\Gamma N_{xs}\left(\frac{dy}{ds}, \frac{dz}{ds}, \frac{2A}{c}\right)ds = (Q_y, Q_z, M_x) \tag{12}$$

where N is the axial force, Q_y and Q_z are the shear forces, M_x is the torsional moment, M_y and M_z are the bending moments, and Q_w is the generalized warping related force (or bimoment). Here q_x, q_y, and q_z are applied, distributed forces, m_x, m_y, and m_z are applied, distributed moments, and q_w is an applied bimoment. The generalized internal forces and the resulting equilibrium equations are identical to those in Ref. 3.

Composite thin-walled construction, herein, is characterized by the membrane stiffness matrix K which relates the non-zero stress resultants to the membrane strains. The constitutive relations are (see also Ref. 1)

$$\begin{aligned} N_{xx} &= K_{11}\epsilon_{xx} + K_{12}\gamma_{xs} \\ N_{xs} &= K_{12}\epsilon_{xx} + K_{22}\gamma_{xs} \end{aligned} \tag{13}$$

The stiffness K_{11} corresponds to uniaxial extension, K_{22} corresponds to shear, and K_{12} is a coupling modulus. They are related to the usual laminate stiffness matrix A (Ref. 9) as follows:

$$\begin{aligned} K_{11} &= A_{11} - \frac{A_{12}^2}{A_{22}} \\ K_{12} &= A_{16} - \frac{A_{12}A_{26}}{A_{22}} \\ K_{22} &= A_{66} - \frac{A_{26}^2}{A_{22}} \end{aligned} \tag{14}$$

For N plies, the laminate stiffnesses are determined by simply adding the plane stress stiffnesses, $\bar{Q}_{ij}$, for each ply. Thus,

$$A_{ij} = \sum_{k=1}^{N} \bar{Q}_{ij}^{(k)}h_k \qquad (i, j = 1, 2, 6) \tag{15}$$

where h_k is the thickness of the kth ply. The ply stiffnesses depend upon the material and fiber orientation.

The deformational variables or generalized strains are easily identified from the strain expressions. Arrayed in a column matrix u they are

$$u = [U_{,x} \quad \gamma_{xy} \quad \gamma_{xz} \quad \phi_{,x} \quad \beta_{y,x} \quad \beta_{z,x} \quad \phi_{,xx}] \tag{16}$$

Similarly the generalized internal forces can be put in a column matrix form as

$$F = [N \quad Q_y \quad Q_z \quad M_x \quad M_y \quad M_z \quad Q_w]^T \tag{17}$$

The relationship between the beam and its reference axis (the coordinate direction x) has not yet been specified; however, it is convenient to choose it in such a way that

$$\begin{aligned} \oint_\Gamma K_{11}yds &= 0 \\ \oint_\Gamma K_{11}zds &= 0 \end{aligned} \tag{18}$$

This choice defines the reference axis as the tension axis found in Ref. 3. This is the axis for which the application of a resultant tensile force will not produce any bending. It is also possible to define the y and z axes as principal flexural axes which uncouple bending about these orthogonal axes in cross section. The necessary condition for this is that

$$\oint_\Gamma K_{11}yzds = 0 \tag{19}$$

Since the force and the deformation are linearly related, a symmetric 7 × 7 stiffness matrix, C, can then be defined such that

$$F = Cu \tag{20}$$

By virtue of the procedure and choice of axes defined above, the elements of C consist of 25 independent stiffness constants

$$C_{11} = \oint_\Gamma K_{11} ds; \quad C_{22} = \oint_\Gamma K_{22} \left(\frac{dy}{ds}\right)^2 ds$$

$$C_{12} = \oint_\Gamma K_{12} \frac{dy}{ds} ds; \quad C_{23} = \oint_\Gamma K_{22} \frac{dy}{ds} \frac{dz}{ds} ds$$

$$C_{13} = \oint_\Gamma K_{12} \frac{dz}{ds} ds; \quad C_{33} = \oint_\Gamma K_{22} \left(\frac{dz}{ds}\right)^2 ds$$

$$C_{14} = \frac{2A}{c} \oint_\Gamma K_{12}\, ds; \quad C_{24} = \frac{2A}{c} \oint_\Gamma K_{22} \frac{dy}{ds} ds$$

$$C_{25} = \oint_\Gamma K_{12} \frac{dy}{ds} z ds; \quad C_{26} = -\oint_\Gamma K_{12} \frac{dy}{ds} y ds$$

$$C_{34} = \frac{2A}{c} \oint_\Gamma K_{22} \frac{dz}{ds} ds; \quad C_{35} = \oint_\Gamma K_{12} \frac{dz}{ds} z ds$$

$$C_{36} = -\oint_\Gamma K_{12} \frac{dz}{ds} y ds; \quad C_{44} = \left(\frac{2A}{c}\right)^2 \oint_\Gamma K_{22} ds$$

$$C_{45} = \frac{2A}{c} \oint_\Gamma K_{12} z ds; \quad C_{46} = -\frac{2A}{c} \oint_\Gamma K_{12} y ds$$

$$C_{55} = \oint_\Gamma K_{11} z^2 ds; \quad C_{66} = \oint_\Gamma K_{11} y^2 ds$$

$$C_{17} = \oint_\Gamma K_{11} \psi ds; \quad C_{27} = \oint_\Gamma K_{12} \frac{dy}{ds} \psi ds$$

$$C_{37} = \oint_\Gamma K_{12} \frac{dz}{ds} \psi ds; \quad C_{47} = \frac{2A}{c} \oint_\Gamma K_{12} y ds$$

$$C_{57} = \oint_\Gamma K_{11} z \psi ds; \quad C_{67} = -\oint_\Gamma K_{11} y \psi ds$$

$$C_{77} = \oint_\Gamma K_{11} \psi^2 ds; \quad C_{56} = -\oint_\Gamma K_{11} yz ds = 0$$

$$C_{15} = \oint_\Gamma K_{11} z ds = C_{16} = -\oint_\Gamma K_{11} y ds = 0 \tag{21}$$

Now that we have the stiffness matrix, it is possible to examine special cases that illustrate some nonclassical effects. In order to apply forces and calculate beam deformations, however, it is necessary to invert Eq. (20) to obtain the flexibility relationship

$$u = SF \tag{22}$$

where $S = C^{-1}$. This inversion is only carried out for certain simplified cases below.

Shear Deformation with Bending-Shear Coupling

The first nonclassical effect examined is that of shear deformation and its coupling with bending. To illustrate this coupling, the terms in the stiffness matrix are evaluated for a circular cross section and a choice of material and fiber orientation so that the extension-twist coupling C_{14} is non-zero. A simple case is that of a slender cantilevered beam with a circular cross section as shown in Fig. 2. For example, consider such a beam with diameter of 2 in and with a circumferentially uniform stiffness (CUS) layup made of IM6/R6376 Graphite/Epoxy. The material properties used in determining the elastic constants are $E_{11} = 23.1 \times 10^6$ psi, $E_{22} = 1.4 \times 10^6$ psi, $\nu_{12} = 0.338$, and $G_{12} = 0.73 \times 10^6$ psi. From these properties and Eq. (21), the 6 × 6 matrix of elastic constants can be determined; the results are presented in Table 1. A blade with these properties is under development at NASA Langley Research Center (Ref. 6).

As can be seen in Table 1, for this type of design there are other nonzero coupling terms (*i.e.*, off-diagonal terms) in addition to C_{14}, which are C_{25} and C_{36}. These terms couple the displacements in the two orthogonal directions by coupling the transverse shear strain along each axis with the bending strain about that axis. The extension, twist, and warping terms are

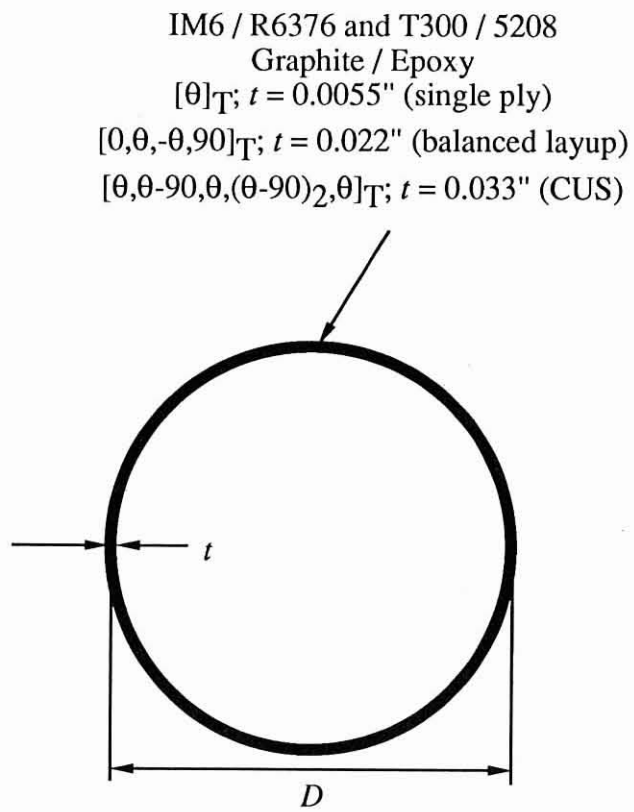

Fig. 2 Schematic of circular tube cross section.

Table 1 Stiffnesses for a composite circular cross section Material IM6/R6376 Graphite/Epoxy $[20, -70, 20, (-70)_2, 20]_T$ Ply thickness 0.0055 in.; D = 2 in.

Stiffnesses	Calculated Values
C_{11}, lb	0.1972×10^7
C_{14}, lb-in	0.6680×10^6
C_{22}, lb	0.2317×10^6
C_{25}, lb-in	-0.3340×10^6
C_{33}, lb	0.2317×10^6
C_{36}, lb-in	-0.3340×10^6
C_{44}, lb-in^2	0.4634×10^6
C_{55}, lb-in^2	0.9862×10^6
C_{66}, lb-in^2	0.9862×10^6

decoupled from these effects; thus, one can consider just the remaining 4 × 4 matrix of stiffness constants so that

$$\begin{Bmatrix} Q_y \\ Q_z \\ M_y \\ M_z \end{Bmatrix} = \begin{bmatrix} C_{22} & 0 & C_{25} & 0 \\ 0 & C_{33} & 0 & C_{36} \\ C_{25} & 0 & C_{55} & 0 \\ 0 & C_{36} & 0 & C_{66} \end{bmatrix} \begin{Bmatrix} \gamma_{xy} \\ \gamma_{xz} \\ \beta_{y,x} \\ \beta_{z,x} \end{Bmatrix} \tag{23}$$

Clearly, now, if one does not consider transverse shear deformation in the model development, as in Refs. 10 and 11 for example, there is no possibility of correctly accounting for the bending-shear coupling terms in Eq. (23). These terms will soften the model, and the question naturally arises whether these coupling effects can be important.

To see the effect more explicitly, consider the inverse of Eq. (23)

$$\begin{Bmatrix} \gamma_{xy} \\ \gamma_{xz} \\ \beta_{y,x} \\ \beta_{z,x} \end{Bmatrix} = \begin{bmatrix} S_{22} & 0 & S_{25} & 0 \\ 0 & S_{33} & 0 & S_{36} \\ S_{25} & 0 & S_{55} & 0 \\ 0 & S_{36} & 0 & S_{66} \end{bmatrix} \begin{Bmatrix} Q_y \\ Q_z \\ M_y \\ M_z \end{Bmatrix} \tag{24}$$

where

$$S_{22} = \frac{1}{C_{22}\left(1 - \frac{C_{25}^2}{C_{22}C_{55}}\right)}; \quad S_{55} = \frac{1}{C_{55}\left(1 - \frac{C_{25}^2}{C_{22}C_{55}}\right)}$$

$$S_{33} = \frac{1}{C_{33}\left(1 - \frac{C_{36}^2}{C_{33}C_{66}}\right)}; \quad S_{66} = \frac{1}{C_{66}\left(1 - \frac{C_{36}^2}{C_{33}C_{66}}\right)}$$

$$S_{25} = \frac{-C_{25}}{1 - \frac{C_{25}^2}{C_{22}C_{55}}}; \quad S_{36} = \frac{-C_{36}}{1 - \frac{C_{36}^2}{C_{33}C_{66}}} \tag{25}$$

Clearly, if one ignores the coupling effect, the transverse shear and bending flexibility coefficients are simply the reciprocals of the transverse shear and bending stiffnesses, respectively, *i.e.*,

$$S_{22} = \frac{1}{C_{22}}; \quad S_{33} = \frac{1}{C_{33}}$$

(coupling ignored)

$$S_{55} = \frac{1}{C_{55}}; \quad S_{66} = \frac{1}{C_{66}} \tag{26}$$

The fact that the correct flexibility coefficients are larger than the ones in which coupling is ignored is now plain.

In order to see the magnitude of the effect we can calculate the deflection of a beam under uniform distributed load in the z direction so that $q_z = q_z^*$ where q_z^* is a constant. From the equilibrium equations, Eqs. (11), and the zero shear force and bending moment boundary conditions at the tip, the shear force and bending moment become

$$Q_y = 0$$

$$Q_z = q_z^*(L - x)$$

$$M_y = -\frac{1}{2} q_z^*(L - x)^2$$

$$M_z = 0 \tag{27}$$

Therefore, from Eqs. (24) the curvature about the y-axis can be written easily in terms of beam flexibility terms and applied loads as

$$\beta_{y,x} = S_{55}M_y = -S_{55}\frac{1}{2} q_z^*(L - x)^2 \tag{28}$$

Integration of Eq. 28 and application of the boundary condition $\beta_y = 0$ at the root yields the section rotation about the y-axis to be

$$\beta_y = \frac{S_{55}q_z^*}{6}[(L - x)^3 - L^3] \tag{29}$$

Now, from the first of Eq. (6)

$$W_{,x} = \gamma_{xz} - \beta_y \tag{30}$$

In light of Eqs. (27) and (24), γ_{xz} can be written in terms of beam flexibility terms and applied loads as

$$\gamma_{xz} = S_{33}Q_z = S_{33}q_z^*(L - x) \tag{31}$$

Substitution of Eq. (31) into Eq. (30) results in

$$W_{,x} = S_{33}q_z^*(L - x) - \frac{S_{55}q_z^*}{6}[(L - x)^3 - L^3] \tag{32}$$

Finally, with the boundary condition that W vanishes at the root, integration of Eq. (32) gives an expression for W

$$W = S_{55}\frac{q_z^*L^4}{24}(\xi^4 - 4\xi^3 + 6\xi^2) + S_{33}\frac{q_z^*L^2}{2}(2\xi - \xi^2) \tag{33}$$

where $\xi = \frac{x}{L}$ and where S_{33} and S_{55} are the correct (including coupling) shear and bending flexibilities, respectively. It can be recognized that the flexibility terms correspond to the engineering flexibility constants found in Ref. 6; S_{55} corresponds to the flapwise bending flexibility, and S_{33} corresponds to the transverse shear flexibility (due to Timoshenko).

To examine a simpler expression, consider only the tip deflection

$$W_{\text{tip}} = \frac{S_{55}q_z^*L^4}{8}\left(1 + \frac{4S_{33}}{S_{55}L^2}\right) \tag{34}$$

The second term in parenthesis corresponds to the direct transverse shear flexibility effect. This term has relative importance only when the ratio $\frac{S_{33}}{S_{55}L^2}$ becomes significant compared to unity; for a beam of given cross sectional geometry and material, this ratio becomes larger as the beam becomes shorter. It may or may not be important for a particular value of slenderness, depending on the ratio of extension and shear moduli. *However, the importance of the elastic coupling—determining the correct values of S_{33} and S_{55}—has nothing to do with slenderness of the beam!* Rather, it depends on the magnitude of the coupling C_{25}^2 relative to $C_{22}C_{55}$. In order to assess this effect, clearly one must determine a complete set of elastic constants (C_{ij}, $i, j = 1, 2, \ldots 6$ at least). The approach of Refs. 10 and 11 will not suffice when the beam is designed for extension-twist coupling.

For a beam whose elastic constants are given in Table 1, Fig. 3 shows the tip deflection determined with two approxi-

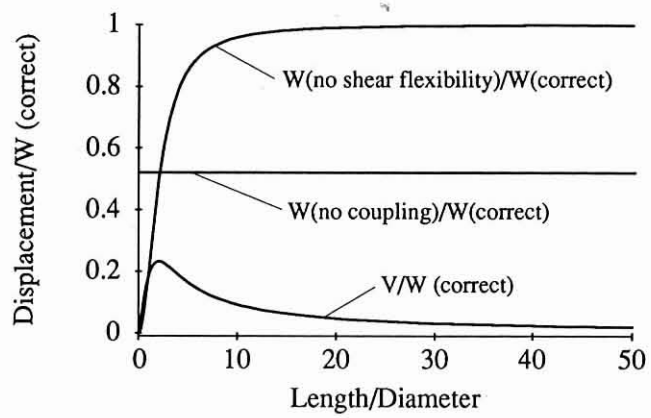

Fig. 3 Effect of beam slenderness on the relative importance of bending-shear coupling and transverse shear flexibility for tip deflection.

mations: (1) without transverse shear flexibility and (2) without bending-shear coupling. Both are normalized by the correct tip deflection from Eq. (34). Neglecting only the direct transverse shear flexibility is seen to be inconsequential for slender beams since, as the length to diameter ratio increases, the normalized displacement tends toward unity. On the other hand, if only the bending-shear coupling is neglected, we see about a 50 percent reduction in the displacement which is independent of the slenderness!

Also shown in Fig. 3 is the lateral displacement V normalized by W. Unless the beam is extremely slender, the presence of bending-shear coupling is seen to induce non-neglible lateral displacements. In light of the importance of the lead-lag deflection and flap-lag elastic coupling in rotor blade stability problems (*e.g.*, see Ref. 12), this would appear to be another reason to include bending-shear coupling.

Fig. 4 shows the magnitude of coupling C_{25}^2 normalized with $C_{22}C_{55}$. (For circular cross sections with constant stiffness around the cross section, this becomes $\frac{C_{25}^2}{C_{22}C_{55}} = \frac{C_{36}^2}{C_{33}C_{66}} = \frac{K_{12}^2}{K_{11}K_{22}} = \beta$.) Here we use the material T300/5208 Graphite/Epoxy with the following properties: $E_{11} = 21.3 \times 10^6$ psi, $E_{22} = 1.6 \times 10^6$ psi, $\nu_{12} = 0.28$, and $G_{12} = 0.9 \times 10^6$ psi. It is seen that the balanced construction does not exhibit any coupling. On the other hand, a single ply gives maximum coupling around

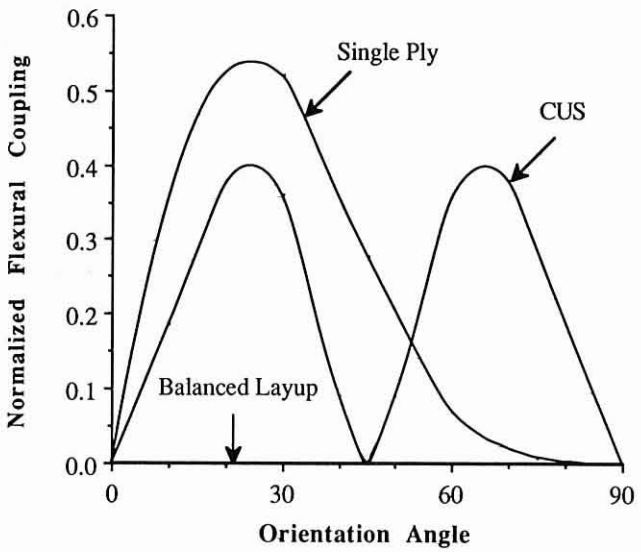

Fig. 4 Variation of normalized bending-shear coupling parameter $\frac{C_{25}^2}{C_{22}C_{55}}$ with respect to ply angle.

$\theta = 23$ deg. Any model which ignores that amount of bending-shear coupling will be off by at least a factor of 2 in predicting the deflections. As θ increases beyond 23 deg the amount of coupling decreases. The CUS construction gives a symmetric distribution about $\theta = 45$ deg at which no coupling exists. The maxima are reached around 23 deg and 67 deg. After its maxima, the amount of coupling decays more rapidly than in the single ply case.

Torsional Warping Rigidity

We now turn to another nonclassical effect, the influence of torsional warping rigidity. In order to proceed, we first need to calculate the solution of the coupled warping-torsion-extension equation. Then, the effect of the warping stiffness on the behavior of a cantilevered box beam will be examined.

Determination of Twist Distribution

Consider a beam subjected to a discrete twisting moment, M_x^*, at the free end with no axial force, implying that $N = 0$. Set $m_x = q_x = q_w = 0$. Taking the twisting moment equilibrium equation, the fourth of Eqs. (11), and writing the moments in terms of kinematical quantities by using the stiffness matrix, one obtains

$$M_x^* = C_T\phi_{,x} - C_{77}\phi_{,xxx} \tag{35}$$

Here the effective torsional stiffness (for zero axial force) is given by

$$C_T = C_{44} - \frac{C_{14}^2}{C_{11}} = C_{44}(1 - \beta) \tag{36}$$

where $\beta = \frac{K_{12}^2}{K_{11}K_{22}}$.

The boundary conditions arise naturally from the principle of virtual work. At $x = 0$ the rotation and warping displacement are restrained so that $\phi = \phi_{,x} = 0$, and at $x = L$ the warping is free so that $\phi_{,xx} = 0$. The classical solution is the particular solution of Eq. (35) or

$$\phi_{cl} = \frac{M_x^*}{C_T}x = \frac{M_x^*L}{C_T}\xi \tag{37}$$

where $\xi = \frac{x}{L}$. With restrained warping, the general solution has the form

$$\phi = \phi_{cl} + \phi_w \tag{38}$$

where the homogeneous solution ϕ_w can be expressed in terms of exponentials

$$\phi_w = C^{(1)}e^{-\lambda\xi} + C^{(2)}e^{\lambda\xi} + C^{(3)} \tag{39}$$

Here λ is a decay length parameter given by

$$\lambda^2 = \frac{C_TL^2}{C_{77}} \tag{40}$$

A large value of λ indicates rapid decay of the solution as the distance from the end increases. Evaluation of the constants from the boundary conditions yields

$$\phi = \frac{M_x^*L}{C_T}\left\{\frac{1}{\lambda(1 + e^{-2\lambda})} \times [e^{-\lambda\xi} - 1 + e^{-2\lambda} - e^{-\lambda}e^{-\lambda(1-\xi)}] + \xi\right\} \tag{41}$$

Assuming that $e^{-\lambda} << 1$ (which is true for practical situations), Eq. (41) reduces to

$$\phi = \frac{M_x^* L}{C_T}\left[\frac{1}{\lambda}(e^{-\lambda\xi} - 1) + \xi\right] \tag{42}$$

It can easily be seen that the tip rotation is

$$\phi\Big|_{\xi=1} = \phi_{cl}\Big|_{\xi=1}\left(1 - \frac{1}{\lambda}\right) \tag{43}$$

Thus, the classical tip rotation is reduced by a factor related to the decay length. If $\lambda >> 1$, then the effect is insignificant; but if λ is, for instance, less than 25, the tip rotation can be significantly reduced.

Influence of Warping Stiffness for Box Beams

Now that the solution is known in terms of λ, we shall determine the value of λ for the cross section under consideration. For the sake of simplicity, suppose that material properties do not change over the cross section. To obtain the effective torsional stiffness, C_T, given in Eq. (36), we use C_{11}, C_{14}, and C_{44} which results in

$$C_T = K_{22}(1 - \beta)\frac{4A^2}{c} \tag{44}$$

For the rectangular cross section (Fig. 5) being used

$$C_T = K_{22}(1 - \beta)16a^3\frac{\alpha^2}{(1 + \alpha)} \tag{45}$$

where $2b$ is the height of the cross section, $2a$ is the width, and $\alpha = b/a$. For the rectangular cross section the warping stiffness becomes

$$C_{77} = K_{11}\frac{4}{3}a^5\frac{\alpha^2(1 - \alpha)^2}{(1 + \alpha)} \tag{46}$$

Thus, λ^2 is then found for the rectangular cross section as

$$\lambda^2 = \frac{K_{22}(1 - \beta)}{K_{11}}\frac{48\sigma^2}{(1 - \alpha)^2} \tag{47}$$

where $\sigma = \frac{L}{2a}$ is a slenderness parameter. The solution for the twist, given in Eq. (42), is identical to that obtained in classical theories for isotropic beams; only the value of the parameter λ is different. Indeed, for isotropic materials one finds that Eq. 47 reduces to

$$\lambda^2 = \frac{G}{E}\frac{48\sigma^2}{(1 - \alpha)^2} \quad \text{(isotropic case)} \tag{48}$$

which agrees with the result obtained by Von Karman and Christensen (Ref. 13).**

**A slightly different result was determined by Benscoter (Ref. 14).

$$\lambda^2 = \frac{G}{E}\frac{48\sigma^2}{(1 + \alpha)^2}$$

The greatest difference between the theories of Refs. 7 and 8 occurs when the cross section is square ($\alpha = 1$), which is the value of α for which the warping displacement and stress vanish at every point in the cross section. A limited numerical study in Ref. 15 suggests that the differences between these two theories are not very great.

It should be observed that λ^2, can be conveniently regarded as a product of "material" and "geometric" parts as long as stiffnesses are uniform around the cross section. Thus, Eq. (47) can be written as

$$\lambda^2 = \lambda_m^2\lambda_g^2$$

$$\lambda_m = \sqrt{\frac{K_{22}(1 - \beta)}{K_{11}}}; \quad \lambda_g = \frac{4\sqrt{3}\sigma}{1 - \alpha} \tag{49}$$

The geometric part, λ_g, is the same for both orthotropic and isotropic beams. However, the material part, λ_m, is different. Figure 6 shows how λ_m changes with fiber orientation. The material used in Fig. 6 is T300/5208 Graphite/Epoxy. In Fig. 7 the variation of λ_g is shown with respect to slenderness parameter and the breadth of the cross section. For a given box beam, the boundary layer parameter can be found by multiplication of the numbers coming from Figs. 6 and 7.

Because λ is relatively large for slender, thin-walled box beams made of isotropic materials, it is well known that the effects of warping are not very important in such beams. For example, a thin-walled beam with the geometry depicted in Fig. 5, with $\frac{E}{G} = 2.5$, $\alpha = 0.25$, and $\sigma = 10$, has $\lambda = 58.42$. Here, warping makes a difference of only 1.7 percent in the tip rotation due to twist.

On the other hand, λ can be much smaller for certain composite beams, giving the "boundary layer" effect more significance. Indeed, for a thin-walled box beam with the same geometry as depicted in Fig. 5, with $\alpha = 0.25$, $\sigma = 10$, and $\theta = 15$ deg, except made of T300/5208 Graphite/Epoxy under "normal" conditions, we obtain $\lambda = 22.35$. In this case, warping makes a difference in the tip rotation due to twist of approximately 4.5 percent. Consider another box beam section with $\alpha = 0.1$, $\sigma = 10$, and $\theta = 0$ deg, made of AS 3501-6 Graphite/Epoxy with hygrothermal effects. The material properties used in the calculation are $E_{11} = 19.3 \times 10^6$ psi, $E_{22} = 0.33 \times 10^6$ psi, $\nu_{12} = 0.41$, and $G_{12} = 0.25 \times 10^6$ psi. Thus, $\lambda = 8.76$, and warping makes a difference in the tip rotation due to twist of approximately 11.4 percent. The classical and nonclassical twist angle predictions and the boundary layer effects for these cases can be seen in Fig. 8; here, thenormalized twist angle is defined as $\frac{\phi C_T}{M_x^* L}$. The boundary layer zone is determined as the distance where the amplitude of the twist rate $\phi_{,\xi}$ is within 5 percent of the classical twist rate (unity).

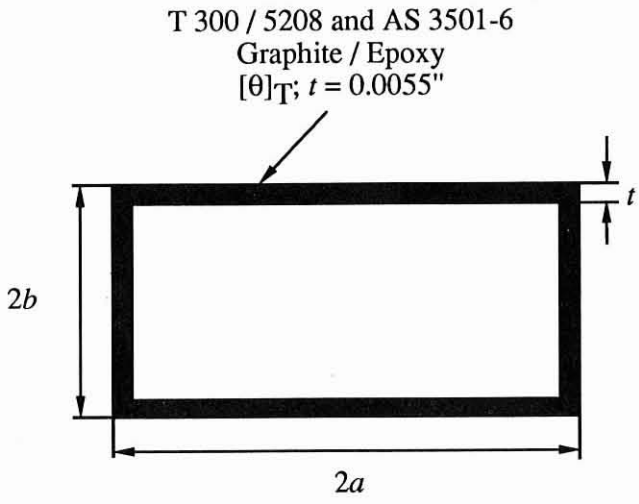

Fig. 5 Schematic of box beam cross section.

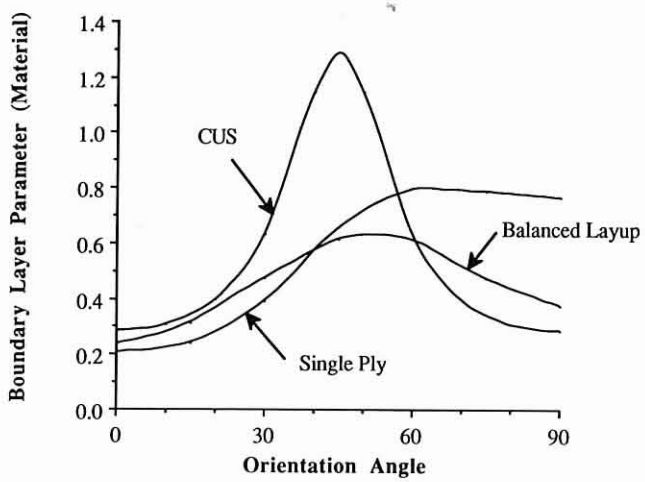

Fig. 6 Variation of material part of the boundary layer parameter λ_m with respect to ply angle.

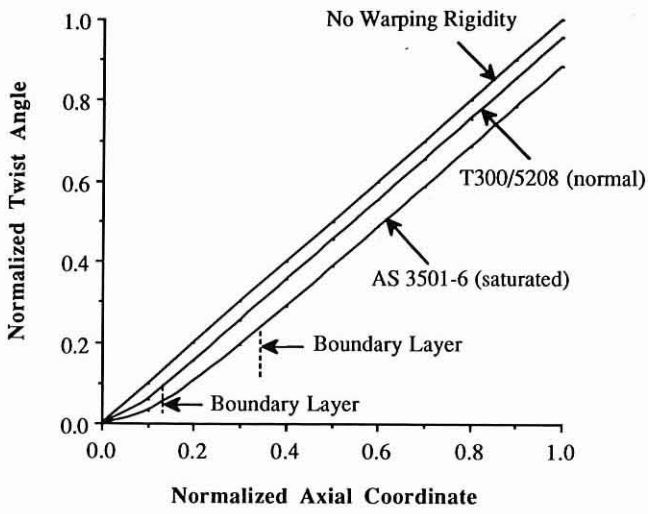

Fig. 8 Variation of normalized twist angle with respect to the axial coordinate for various values of λ.

The percentage reduction in twist angle at the tip increases for beams for smaller values of α. We hereby conclude from this that restrained torsional warping can affect certain global deformation results. Extremely small values of such parameters as the slenderness $L/2a$, the thickness ratio α, the material ratio K_{22}/K_{11}, and ply angle θ being chosen to give a small λ_m can result in a value for λ that influences the tip rotation in a significant way. Thus, this effect should be weighed carefully before being excluded from composite rotor blade analyses.

Concluding Remarks

Two main conclusions have been drawn in the present work:

1. In structural models designed for extension-twist coupling (the circumferentially uniform stiffness case), an important degree of bending-shear coupling is present which causes the structure to be significantly more flexible in bending than it would be if the coupling were ignored. In light of possible uses of extension-twist coupling in future designs, effects such as coupling between bending and shear deformation must be present in any general-purpose analysis. It is further observed that, without the presence of shear deformation in the kinematics, the proper form of the coupling terms in the flexibility matrix cannot be obtained. The influence of this coupling is far more significant in the case analyzed than the direct (Timoshenko) effect of transverse shear flexibility and is independent of the slenderness of the beam. This coupling also induces an elastic "flap-lag" type coupling the influence of which on rotor blade stability is well known. Finally, even the direct shear flexibility term may not be negligible for the composite case in general, because there are materials for which the shear modulus may be much smaller than the extension modulus (*i.e.*, $K_{22} << K_{11}$).

2. Torsional warping is found to be significant enough to warrant its inclusion in composite beam analyses in certain circumstances. A boundary layer parameter caused by the restrained warping at the ends is identified. Although this parameter is relatively large for slender, thin-walled beams made of isotropic materials, it can be much smaller for composite beams. A smaller boundary layer parameter yields longer decay length, along which the end effects prevail and stiffen the structure. Thus, the smaller this parameter the larger the error in the twist angle predictions. In some rather unusual cases, the error in the twist angle predictions at the tip can reach more than 10 percent. Therefore, inclusion in the cross sectional stiffness matrix of the torsional warping rigidity, which stems from the inclusion of an additional variable to the kinematical field, would be important for certain laminated structures.

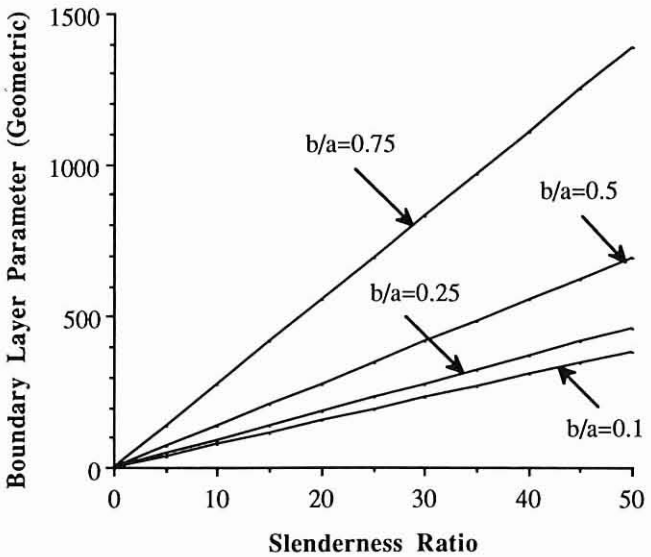

Fig. 7 Variation of geometric part of the boundary layer parameter λ_g with respect to ply angle.

Acknowledgments

This work was supported by the U.S. Army Research Office under contracts DAAG29-82-K-0094 and DAAL03-88-C-0003.

References

[1]Hodges, D. H., "Review of Composite Rotor Blade Modeling," *AIAA Journal*, Vol. 28, (3), 1990.

[2]Giavotto, V., *et al.*, 1983, "Anisotropic Beam Theory and Applications," *Computers and Structures*, Vol. 16.

[3]Rehfield, L. W., "Design Analysis Methodology for Composite Rotor Blades," *Proceedings of the 7th DoD/NASA Conference on Fibrous Composites in Structural Design*, (V(a)-1)–(V(a)-15), 1985.

[4]Bauchau, O. A., "A Beam Theory for Anisotropic Materials," *Journal of Applied Mechanics*, Vol. 52, (2), 1985.

[5]Hodges, D. H., Atilgan, A. R., Fulton, M. V., and Rehfield, L. W.,

"Dynamic Characteristics of Composite Beam Structures," *Proceedings of the American Helicopter Society National Specialists' Meeting on Rotorcraft Dynamics*, Arlington, Tex., Nov 13–14, 1989.

[6]Hodges, R. V., Nixon, M. W., and Rehfield, L. W., "Comparison of Composite Rotor Blade Models: A Coupled Beam Analysis and an MSC/NASTRAN Finite Element Model," NASA Technical Memorandum 89024, 1987.

[7]Bauchau, O., Coffenberry, B. S., and Rehfield, L. W., "Composite Box Beam Analysis: Theory and Experiments," *Journal of Reinforced Plastics and Composites*, Vol. 6, (1), 1987.

[8]Nixon, M. W., "Extension-Twist Coupling of Composite Circular Tubes with Application to Tilt Rotor Blade Design," *Proceedings of the 28th Structures, Structural Dynamics, and Materials Conference*, Apr 6–8, 1987, Monterey, Calif., AIAA Paper No. 87-0772.

[9]Jones, R. M., *Mechanics of Composite Materials*, McGraw Hill, 1975.

[10]Mansfield, E. H., and Sobey, A. J., "The Fiber Composite Helicopter Blade—Part 1: Stiffness Properties—Part 2: Prospects for Aeroelastic Tailoring," *Aeronautical Quarterly*, Vol. 30, (2), 1979.

[11]Hong, C.-H., and Chopra, I., "Aeroelastic Stability of a Composite Blade," *Journal of the American Helicopter Society*, Vol. 30, (2), 1985.

[12]Ormiston, R. A., "Concepts for Improving Hingeless Rotor Stability," *Proceedings of the American Helicopter Society Mideast Region Symposium of Rotor Technology*, Essington, Pennsylvania, Aug 1976.

[13]Von Karman, T., and Christensen, N. B., "Methods of Analysis for Torsion with Variable Twist," *Journal of Aerornautical Science*, Vol. 11, (11), 1944.

[14]Benscoter, A. U., "A Theory of Torsion Bending for Multi-Cell Beams," *Journal of Applied Mechanics*, Vol. 21, (1), 1954.

[15]Murray, N. M., *Introduction to the Theory of Thin-Walled Structures*, Oxford Science Publishers, 1985.